Characteristics of axial-type HTS motor under different temperature conditions

AUTHOR(S):

Jung, HJ; Nakamura, T; Muta, I; Hoshino, T

CITATION:

Jung, HJ ...[et al]. Characteristics of axial-type HTS motor under different temperature conditions. IEEE TRANSACTIONS ON APPLIED SUPERCONDUCTIVITY 2003, 13(2): 2201-2205

ISSUE DATE:

2003-06

URL:

http://hdl.handle.net/2433/39950

Characteristics of Axial-Type HTS Motor Under Different Temperature Conditions

Hun-June Jung, Taketsune Nakamura, Itsuya Muta, and Tsutomu Hoshino

***Abstract*—We tested an axial-type Bi-2223 bulk motor under different magnetic field and temperature conditions. Distributed armature windings with a pole number of four were used in order to compensate for the harmonic components in the air-gap magnetic flux density. The temperature was varied by evacuating the metal cryostat with a rotary vacuum pump. The fabricated motor demonstrated hysteresis characteristics when the temperature of the system was decreased and the magnetomotive force was adjusted to appropriate values. Then, synchronous speed at no-load condition was fulfilled. On the other hand, slip of rotational speed as well as inductive torque was induced when temperature and magnetic conditions were not satisfied. These results can be explained based on the pinning properties and AC loss inside the bulk rotor.**

***Index Terms*—Bi-2223, bulk motor, hysteresis torque, induction torque, synchronous speed.**

I. Introduction

In THE past several years, there has been increasing interest in bulk high temperature superconductor (HTS) because of improvements of manufacturing techniques as well as material properties. Then, some power applications of HTS bulk materials have been proposed and studied in order to increase power densities and reduce energy losses. As one of such applications, several types of electrical motor, i.e., hysteresis, reluctance and trapped field motor etc., have been studied [1], [2], [3], [4], [5].

In most studies of HTS bulk motors, YBCO bulk materials have been used as the rotor due to its strong flux pinning. On the other hand, we have considered other materials for motor applications. For one of the candidate materials, we have fabricated and tested an axial-type motor using a Bi-2223 bulk rotor [6], [7], [8]. The fabricated motor, however, has not reached synchronous speed, and large slippage occurred. Furthermore, motor characteristics have shown inductive behaviors with large resistance.

There are mainly two reasons for the aforementioned properties [9]. The first reason can be attributed to the structure of the armature windings. Salient and concentrated windings were used for the armature, and then the resulting flux distribution contained large space harmonics [10]. It is known that the harmonic components influence the motor characteristics, and asynchronous torque is generated.

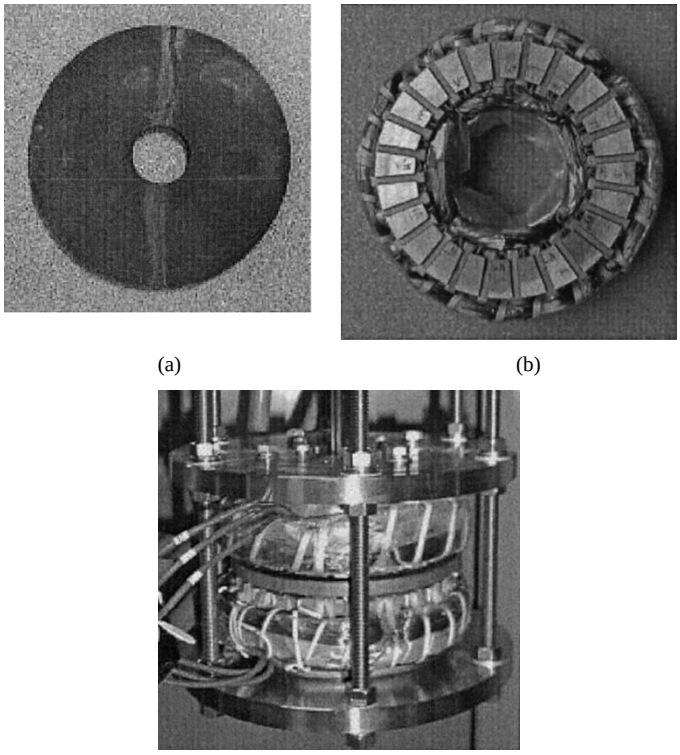

(a) (b) (c)

Fig. 1. Photographs of axial-type Bi-2223 bulk motor. (a) Bi-2223 bulk rotor (120 mm^{OD}, 26 mm^{ID}, 7 mm^{H}). (b) 4-pole and 24-slot stator with distributed winding. (c) Assembled axial-type Bi-2223 bulk motor.

The second reason is the weak pinning property of Bi-2223 bulk at high temperatures such as 77.3 K. McCulloch *et al.* carried out a comparative study of Bi-2212 and YBCO motors [11]. According to their study, although the YBCO motor was operated with synchronous speed, the Bi-2212 motor did not reach at the same condition.

In this paper, we deal with the aforementioned problems. The distributed windings are introduced in order to reduce the space harmonics of air-gap magnetic flux density. The distribution of the magnetic flux density is measured by Hall sensor and analyzed by Fast Fourier Transform (FFT). The performance of the fabricated motor is evaluated by locked rotor, no load and load tests. Furthermore, the tests are also performed at different temperatures in order to examine the relationship between the torque generation and the pinning properties of a Bi-2223 bulk rotor.

Manuscript received August 6, 2002. This work was supported in part by Grant-In-Aid for Scientific Research (no. 13450113) from The Ministry of Education, Culture, Sports, Science and Technology, Japan.

The authors are with the Graduate School of Engineering, Kyoto University, Yoshida Honmachi, Sakyo, Kyoto 606-8501, Japan (e-mail: hjjung@asl.kuee.kyoto-u.ac.jp; hoshino@asl.kuee.kyoto-u.ac.jp; tk_naka@kuee.kyoto-u.ac.jp; muta@kuee.kyoto-u.ac.jp).

Digital Object Identifier 10.1109/TASC.2003.813036

II. Experimental

A. Structure of Axial-Type Bi-2223 Bulk Motor

Photographs of the fabricated axial-type Bi-2223 bulk motor are shown in Fig. 1. A $Bi_{1.85}Pb_{0.35}Sr_{1.90}Ca_{2.05}Cu_{3.05}O_X$ (Bi-2223) disk, 120 mm in outer diameter, 26 mm in inner diameter and 7 mm in height, is used for the rotor [Fig. 1(a)]. The crystallographic c-axis of the disk is oriented perpendicular to the disk surface. The critical current density defined with the electric field criterion of 10^{-4} Vm^{-1}, J_c, and critical temperature, T_c, are, respectively, 3×10^7 A/m^2 (at 77.3 K, self-field) and 105 K. Because the bulk rotor was broken during the last experiment, two segments were glued together using epoxy resin as shown by white shades in Fig. 1(a). It was confirmed that the motor characteristics were not effected by the accident.

We use a stator with distributed winding in a 24 semi-enclosed slot structure [Fig. 1(b)]. The dimensions of the stator are 116.4 mm, 71.4 mm and 41.4 mm for outer diameter, inner diameter and height, respectively. The armature winding is wound with 3-phase and 4-pole, then each phase is connected in wye. As shown in Fig. 1(c), the bulk rotor is sandwiched in between two stators that are connected in parallel to each other.

B. Measurement Method of Air-Gap Flux Density Distribution

The distribution of magnetic flux density in the air-gap of the motor is measured as a function of time in order to see the space harmonics. A rotating magnetic field with a speed of 1800 rpm is generated in the air-gap by the stator. The air-gap flux density is measured by a transverse type Hall sensor that is mounted on the rotor surface. The measurements are performed from the center of the phase-a slot to that of the phase-c slot at intervals of 1°.

C. Test Method of Axial-Type HTS Motor

Locked rotor, no load and load tests are carried out by varying the temperature. All the tests are performed with the system that is immersed in liquid nitrogen with zero field cooling method. In order to vary the temperature of the system, evaporated nitrogen gas is pumped out by a rotary vacuum pump. The measurement apparatus is connected to a motor that is installed into the metal cryostat through the ferro-fluid seal. The load is applied with a micropowder brake, and the torque as well as the rotational speed is measured by a contactless torque meter.

III. Air-Gap Flux Density Distribution

Fig. 2(a) shows the spatial distribution of magnetic flux density in the air-gap at room temperature. The center of phase-a slot is set to be $\theta_m = 0$. The electrical angle of phase-a is 0°. The corresponding amplitude of the space harmonics obtained by Fast Fourier Transform (FFT) is also shown in Fig. 2(b). As can be seen, the spatial distribution is almost sinusoidal except for small harmonic components such as 11th and 13th orders.

The same measurements were also performed in liquid nitrogen (77.3 K) in order to examine the effect of the superconducting Bi-2223 bulk rotor upon the spatial distribution of the air-gap magnetic flux density. The measured results are shown in Fig. 3 for three different armature currents. Under the condition of $I_a = 1$ A, no definite rotating field is observed due to the shielding property of the bulk. In this condition, there is no torque generation. This will be discussed later. As the armature current is increased, however, the magnetic flux is beginning to penetrate into the bulk rotor. Thus, one can observe the rotating field [Fig. 3(b) and (c)]. Comparing Figs. 2(a) and 3(b), one can see the phase difference between the flux distribution at room temperature and that at 77.3 K due to the hysteretic property of the superconducting rotor. This phase difference is the origin of the hysteresis torque generation. Table I lists the amplitude of harmonics normalized by the fundamental component. Harmonic components of 11th and 13th orders are more induced at 1 A and 77.3 K than any other current value, due to the shielding property of the bulk. As the armature current increases, however, these harmonic components are reduced.

TABLE I
Harmonic Components of Air-Gap Flux Distribution

Order	Ratio			
	2A, R.T.	1A, 77.3K	2A,77.3K	4A, 77.3K
1	1	1	1	1
5	0.0652	0.3062	0.0780	0.0664
7	0.0459	0.4535	0.0791	0.0569
11	0.1743	0.9280	0.1745	0.1458
13	0.0782	1.3256	0.1678	0.0996
23	0.0689	0.5814	0.0802	0.0751
25	0.0176	0.6667	0.0660	0.0335

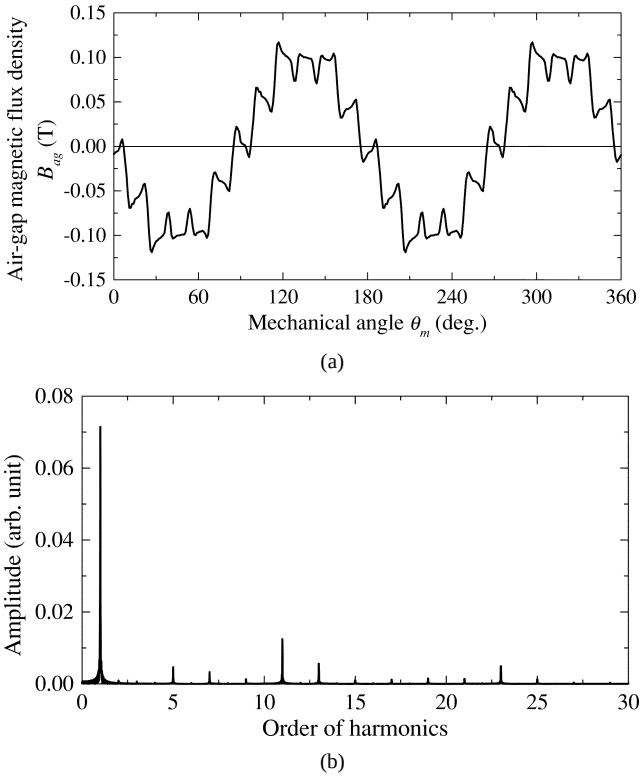

Fig. 2. Air-gap flux distribution and harmonic components at room temperature. Armature current, I_a, is 2.0 A. (a) Air-gap flux distribution. (b) Amplitude of space harmonics.

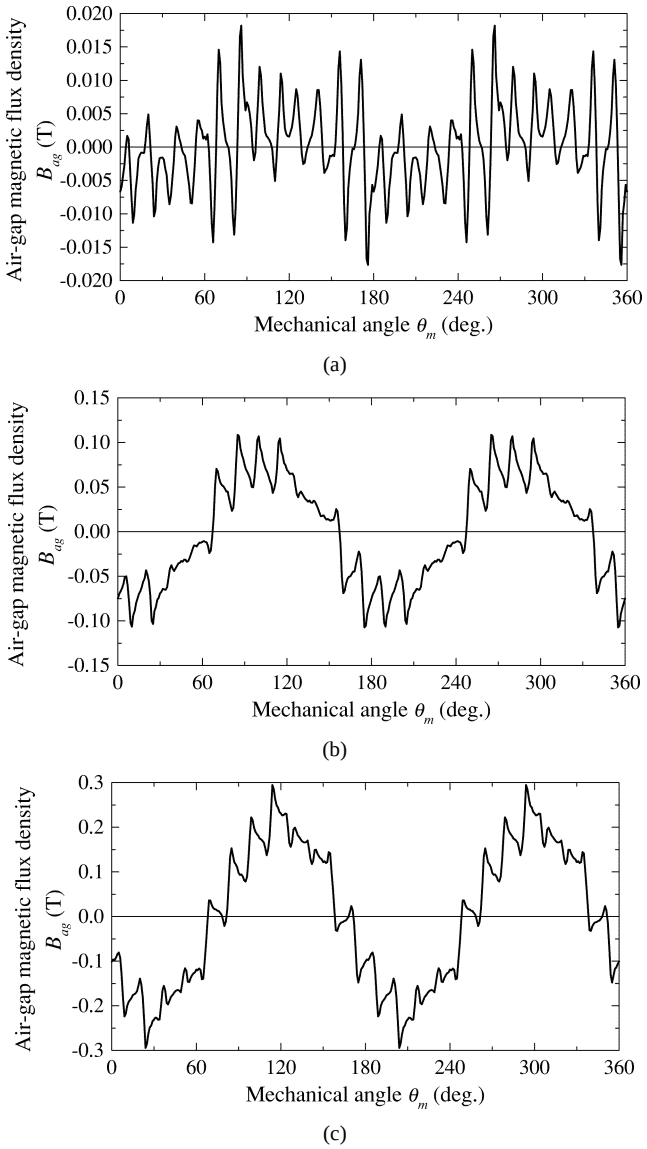

Fig. 3. Air-gap magnetic flux distribution at 77.3 K. (a) $I_{\rm a} = 1.0$ A. (b) $I_{\rm a} = 2.0$ A. (c) $I_{\rm a} = 4.0$ A.

IV. Performance Evaluation of Axial-Type Bi-2223 Bulk Motor

A. Locked Rotor Test

Torque, τ, vs. armature current, $I_{\rm a}$, characteristics are measured under the condition that the rotor shaft is fixed by the powder brake. In order to understand the effect of the hysteresis properties of Bi-2223 bulk rotor on the torque generation, tests are performed at different temperatures from 64.0 K to 77.3 K as shown in Fig. 4. The plots with double logarithmic scale are also shown in the inset. The torques are generated around 1 A of armature current. These results are reasonably consistent with those of air-gap flux density measurements, i.e., there is almost no rotating field generated below this current.

Although a small discrepancy occurs at 77.3 K, the temperature dependent τ vs. $I_{\rm a}$ curves intersect at around 3.5 A. The curvature of these curves change at this current. Barnes *et al.* pointed out by finite difference modeling based on critical state model that the magnetic flux has fully penetrated at the point

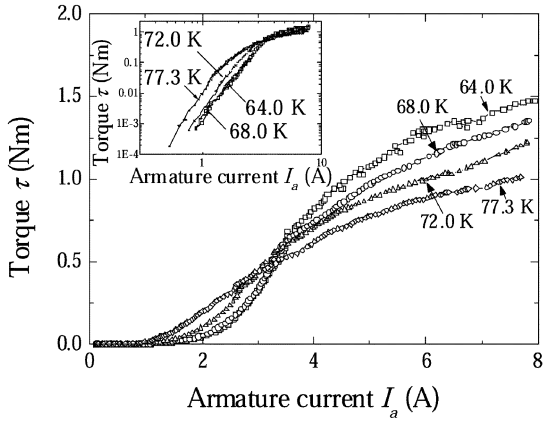

Fig. 4. Torque, τ, versus armature current, I_a, curves for different temperatures. Inset: Double logarithmic plots.

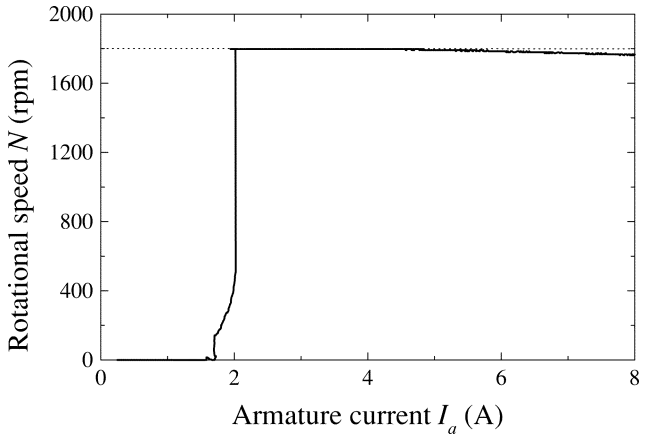

Fig. 5. No load speed variation against armature current at $T = 64.0$ K.

that the curvature changes [13]. It can be deduced that the same phenomenon also occurs in this case. Furthermore, it is interesting to point out that the opposite temperature dependencies are observed between below and above this current. That is, the pinning characteristics of superconducting Bi-2223 bulk is surely increased by lowering the temperature. Then, most of the rotating field is shielded when the armature current is lower than 3.5 A. On the other hand, after the flux is fully penetrated into the bulk, i.e., $I_{\rm a} > 3.5$ A, the lower the temperature is, the larger the generated torque is, due to the improvement of flux trapping capability.

B. No Load Test

First, a no load test was performed at 77.3 K. The rotational speed, however, did not reach a synchronous speed (1800 rpm), and a small slip, e.g., 0.06 at 4 A, is induced. As shown in Fig. 2, the rotating field is almost sinusoidal. Therefore, we consider that the reason for this slip comes from the bulk rotor's property, i.e., penetrated flux flows in the bulk due to the weak pinning. Then, the same test is performed at lower temperature in order to examine this consideration. Fig. 5 shows the rotational speed, N, vs. armature current, $I_{\rm a}$, characteristics at 64.0 K. As can be clearly seen, the rotational speed exactly reaches the synchronous one. On the other hand, the speed also begins to decrease at $I_{\rm a} > 4.4$ A, and this may be due to the flux

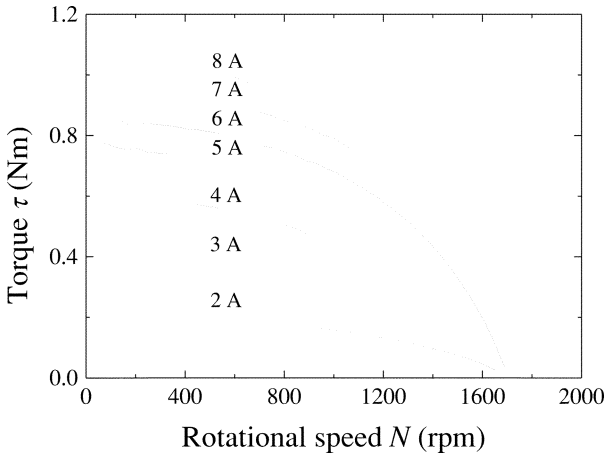

Fig. 6. Torque, τ, vs. rotational speed, N, curves for different armature currents at 77.3 K.

flow. Namely, the flux flow produced inductive properties in the rotor, and then the speed of the motor was decreased. Therefore, synchronous speed is only realized at the current range of 2 A $< I_{\rm a} <$ 4.4 A, for 64.0 K. These characteristics are also confirmed by the load test results that is presented in the next subsection.

C. Load Test

Fig. 6 shows τ vs. N curves for different armature currents at 77.3 K. Generated torque increases as the current, and reaches over 1 Nm at 8 A. However, the synchronous speed (1800 rpm) is not obtained even under a no load condition. As can be seen, the motor shows characteristics of an induction motor with large rotor resistance.

Then, the same measurements are carried out at decreasing temperatures. Results are shown for armature currents of (a) 1.5 A, (b) 4.0 A and (b) 8.0 A, in Fig. 7. Opposite temperature dependences are observed as compared between (a) and (b) [or (c)]. These results are consistent with those of the locked rotor test. On the other hand, it has to be emphasized that the hysteresis like characteristic is observed at 64.0 K and 4.0 A as shown in Fig. 7(b). That is, the motor produces an almost constant torque up to almost synchronous speed, and then reaches synchronous speed. Therefore, a Bi-2223 motor can become a hysteresis motor only at lower temperatures and appropriate range of armature current. Under the other conditions, the motor shows inductive characteristics.

V. Conclusions

We fabricated and tested an axial-type Bi-2223 bulk motor that has distributed armature windings. The characteristics of the motor were improved compared with those of the previous motor that has salient and concentrated armature windings. Based on the locked rotor, no load and load tests, temperature dependence of the motor characteristics are clarified. That is, the lower the temperature is, the smaller the generated torque is, due to the shielding properties of the Bi-2223 bulk at smaller armature current. On the other hand, when the flux is fully penetrated by the large armature current, opposite temperature dependency is observed due to the increasing flux pinning property. Furthermore, it was found for the first time that the motor shows hysteresis characteristics at the lower temperature and appropriate range of armature current.

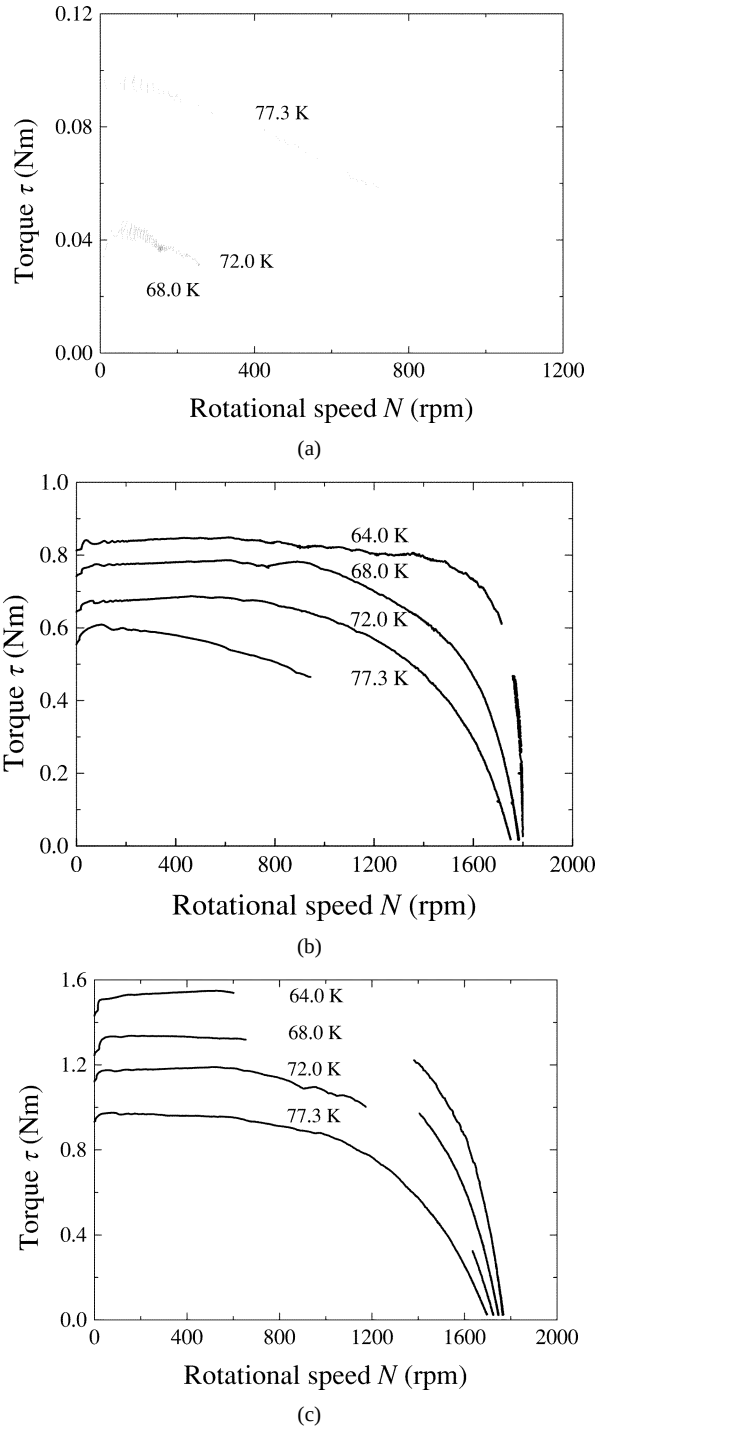

Fig. 7. Torque, τ, vs. rotational speed, N, curves for different temperatures. Rotational speed N (rpm) (a) $I_{\rm a} = 1.5$ A. (b) $I_{\rm a} = 4.0$ A. (c) $I_{\rm a} = 8.0$ A.

References

[1] L. K. Kovalev, K. V. Ilushin, V. T. Penkin, K. L. Kovalev, S. M.-A. Koneev, V. N. Poltavets, A. E. Larionoff, K. A. Modestov, S. A. Larionoff, W. Gawalek, T. Habisreuther, B. Oswald, K.-J. Best, and T. Strasser, "Hysteresis and reluctance electric machines with bulk HTS elements. Recent results and future development," *Superconductor Science and Technology*, vol. 13, pp. 498–502, 2000.

[2] G. J. Barnes, M. D. McCulloch, and D. Dew-Hughes, "Applications and modeling of bulk HTS's in brushless AC machines," *Superconductor Science and Technology*, vol. 13, pp. 875–878, 2001.
[3] L. K. Kovalev, K. V. Ilushin, V. T. Penkin, K. L. Kovalev, S. M.-A. Koneev, K. A. Modestov, S. A. Larionoff, W. Gawalek, and B. Oswald, "HTS electrical machines with YBCO bulk and Ag-BSCCO plate-shape HTS elements: Recent results and future development," *Physica C*, vol. 354, pp. 34–39, 2001.
[4] ——, "Electrical machines with bulk HTS elements," *Physica C*, vol. 357, pp. 860–865, 2001.
[5] H. Ohsaki and Y. Tsuboi, "Study on electric motors with bulk superconductors in the rotor," *Journal of Materials Processing Technology*, vol. 108, pp. 148–151, 2001.
[6] I. Muta, H. J. Jung, T. Hirata, T. Nakamura, T. Hoshino, and T. Konishi, "Fundamental experiments of axial-type BSCCO-bulk superconducting motor model," *IEEE Transactions on Applied Superconductivity*, vol. 11, no. 1, pp. 1964–1967, 2001.
[7] I. Muta, T. Nakamura, T. Hirata, T. Hoshino, and T. Konishi, "Preliminary study on axial-type BSCCO superconducting motor," *Physica C*, vol. 54, pp. 100–104, 2001.
[8] I. Muta, H. J. Jung, T. Nakamura, and T. Hoshino, "Performance of axial-type motor with Bi-2223 HTS bulk rotor," *Physica C*, vol. 372–375, pp. 1535–1538, 2002.
[9] T. Nakamura, I. Muta, H. J. Jung, and T. Hoshino, "Electromagnetic characteristics of axial-type HTS motor utilizing Bi-2223 bulk rotor" (in Japanese), *Cryogenic Engineering*, vol. 37, no. 11, pp. 726–733, 2002.
[10] I. Muta, H. J. Jung, T. Nakamura, and T. Hoshino, "Performances of axial-type superconducting BSCCO-2223 motor," in *Proceedings of ICEM 2002*, 2002, pp. 190–195.
[11] M. D. McCulloch, K. Jim, K. Kawai, and D. Dew-Hughes, "Prospects for brushless AC machines with HTS rotors," in *Inst. Phys. Conf. Ser.*, 1997, No. 158, pp. 1519–1522.
[12] T. Nakamura, K. Fukui, H. J. Jung, I. Muta, and T. Hoshino, "Investigation of magnetic characteristics in HTS bulk materials for motor application," in *Preprint of Applied Superconductivity Conference 2002*, 2002.
[13] G. J. Barnes, M. D. McCulloch, and D. Dew-Hughes, "Finite difference modeling of bulk high temperature superconducting cylindrical hysteresis machines," *Superconductor Science and Technology*, vol. 13, pp. 229–236, 2000.